Supplementary Information (SI) for Environmental Science: Processes & Impacts.

Supporting Information of

Atmospheric aging suppresses the formation of limonene-derived organic peroxides

Xiaowen Chen,[a] Yunyan Zhao,[b] Shan Zhang,[a] Lin Du [abc] and Kun Li *[a]

[a] Qingdao Key Laboratory for Prevention and Control of Atmospheric Pollution in Coastal Cities, Environment Research Institute, Shandong University, Qingdao, 266237, China

[b] School of Environmental Science and Engineering, Shandong University, Qingdao, 266237, China

[c] State Key Laboratory of Microbial Technology, Shandong University, Qingdao, 266237, China

**Correspondence to*: Kun Li (email: kun.li@sdu.edu.cn)

(18 Pages, 4 Texts, 4 Figures, 5 Tables)

Text S1 OFR calculation

Equivalent photochemical age calculation

In all OFR experiments, we used equivalent photochemical age to standardize the OH concentration during photooxidation. It is assumed that the average atmospheric OH concentration of 1 day is 1.5×10^6 molecules cm^{-3}.[1] The term $[OH]_{exp}$ (expressed in molecules cm^{-3} s) is used to characterize the integrated OH concentration within the OFR system. It represents the product of the instantaneous OH concentration (molecules cm^{-3}) and the mean residence time (s). To indirectly quantify OH exposure and equivalent photochemical ages under concurrent conditions of VOCs, O_3, and UV irradiation, a controlled CO introduction method was employed. This approach leverages the well-defined reaction kinetics between CO and OH radicals:

$$OH_{exp} = -\frac{1}{k_{CO}} \ln \frac{[CO]_t}{[CO]_0} \tag{S1}$$

Where the second-order rate constant for the CO and OH reaction at 298 K (1.54×10^{-13} cm^3 $molecules^{-1}$ s^{-1}), was adopted as based on established literature.[2] The initial CO concentration ($[CO]_0$), measured by a calibrated CO monitor after system stabilization (> 30 min) without UV illumination, was set at approximately ~3 ppm. The final steady-state CO concentration ($[CO]_t$) was determined under UV irradiation following an equivalent stabilization period (> 30 min).

The ratio of reacted VOCs with OH and O_3

$$R = \frac{k_{OH\times VOC} \times [OH]}{k_{O3\times VOC} \times [O_3]} \tag{S2}$$

where R is the ratio of pathways in which VOC reacts with OH or O_3, respectively. The $k_{OH\times VOC}$ (1.64×10^{-10} cm^3 $molecule^{-1}$ s^{-1}) and $k_{O3\times VOC}$ (2.1×10^{-16} cm^3 $molecule^{-1}$ s^{-1}) is the second-order rate constant of styrene with OH and VOCs with O_3, respectively.[3] [OH] and $[O_3]$ is the OH concentration and O_3 concentration in the OFR.

SOA yield

The SOA yield (Y) for organic gas can be calculated as:

$$Y = \frac{\Delta M}{\Delta HC} \tag{S3}$$

Where the ΔM is the total mass concentration of SOA that can be measured by SMPS, it is noted that the SOA mass concentration was calculated from the volume concentration measured with SMPS and the aerosol density. The density of limonene SOA was estimated to be 1.25 g cm^{-3}.

Text S2 Potential OFR limitations

In this study, we used an OFR254 flow reactor to simulate atmospheric oxidation conditions, with ozone concentrations maintained at approximately 3 ppm, relative humidity around 40%, and an OH reactivity (OHR) of up to 1500 s^{-1} when VOC concentration was high. The ozone concentration and relative humidity in our setup are selected to reduce non-OH oxidation pathways while still maintaining realistic atmospheric conditions. The relatively high humidity (around 40%) helps simulate tropospheric moisture levels but may weaken the role of non-OH oxidants, such as O_3, $O(^1D)$, and $O(^3P)$, in VOC oxidation. At the same time, the low ozone concentration (~3 ppm) minimizes the interference of non-OH reaction pathways, ensuring that OH remains the dominant oxidant. While the high OHR reflects elevated precursor concentrations, the controlled humidity and ozone levels provide a reasonable simulation of OH-dominated atmospheric oxidation processes.[4]

One important consideration is the potential divergence of peroxy radical (RO_2) chemistry. Under low-NO_x conditions, the OH/HO_2 ratio may be higher than in typical ambient conditions, leading to a greater role for RO_2 + OH reactions. This, combined with shorter RO_2 lifetimes due to higher radical concentrations in the OFR, could limit the relevance of the observed chemistry to the troposphere.

Given these limitations, it is important to interpret results with caution when simulating high photochemical ages, particularly beyond one week. However, there is currently no ideal method for accurately replicating extended atmospheric aging processes, making OFRs a valuable tool despite their limitations when studying atmospheric oxidation chemistry.

Text S3 Experimental details

GC-FID

The concentration of limonene was monitored using gas chromatography (GC) equipped with a flame ionization detector (FID) and a DB-624 capillary column (30 m × 0.32 mm, 1.8 μm film thickness; Agilent Technologies, USA) until stabilization was achieved. The GC oven temperature program was as follows: initial temperature 80 °C, ramped at 20 °C min^{-1} to 180 °C, and held at 180 °C for 2 min.

SMPS

During SOA generation, the particle size distribution, volume concentration, and number concentration were monitored online using a Scanning Mobility Particle Sizer (SMPS, Model 5416, Grimm Aerosol Technik, Germany). The SMPS system consists of a Differential Mobility Analyzer (DMA) and a Condensation Particle Counter (CPC). Measurements were performed every 10 minutes. The aerosol sample flow rate and sheath air flow rate were maintained at 0.3 L min^{-1} and 3.0 L min^{-1}, respectively, covering a mobility diameter range of 13.8 to 723.4 nm.

Iodometry assay

For analysis, SOA filter samples were first ultrasonically extracted for 20 min using 5 mL of methanol (Optima® LC-MS grade, Fisher Scientific). The sonication was conducted in an ice bath to prevent heat generated during the process from causing peroxide decomposition. The extract was filtered through a PTFE membrane (0.22 μm pore size). The filtrate was then concentrated to 500 μL under a gentle nitrogen stream. A 200 μL aliquot of the concentrated extract was mixed with 400 μL of pH = 3 acetic acid aqueous solution in a sealed vial. The mixture was purged with high-purity nitrogen gas for 3 min to remove dissolved oxygen. While nitrogen bubbling continued, 30 μL of 1.2 mol L^{-1} KI aqueous solution was injected under a slight positive nitrogen pressure. The solution was reacted in the dark at room temperature for 1 h, during which KI reacted with peroxides in the sample under oxygen-free, acidic, and light-excluded conditions, generating the stable chromophore I_3^- for UV spectrophotometric determination. A separate 200 μL aliquot of the SOA concentrate underwent identical processing but without KI addition to serve as a blank. Subsequently, 150 μL of each mixture (KI-reacted and blank) was transferred into autosampler vials equipped with inserts for mass spectrometric analysis. For the iodometric assay, an additional 150 μL aliquot of the KI-reacted mixture was placed into a chromatographic vial after the 1 h reaction, with the remainder reserved for UV analysis.

Solution absorbance was measured across the 200-850 nm range using a UV-Vis spectrophotometer. The absorbance at 351 nm (λ_{max} for I_3^-) exhibited a linear correlation with peroxide concentration. Relative quantification was performed by constructing a linear calibration curve using a series of hydrogen peroxide solutions (30 wt.%), measuring their absorbance at 350 nm. This enabled the quantification of the total peroxide concentration in the particulate matter, expressed as H_2O_2 equivalents (H_2O_{2eq}). These results were used for subsequent peroxide yield calculations.

KI solution preparation: Dissolved oxygen must be thoroughly removed during KI solution preparation. The specific procedure is: Add 3 mL of ultrapure water to an amber vial, purge with high-purity nitrogen gas for 3 minutes to effectively remove dissolved oxygen. Precisely weigh 600 mg of KI powder and add it to the ultrapure water under continuous nitrogen purging to prepare the KI solution (1.2 M). Seal the solution immediately and use it within 2 hours. Discard and freshly prepare if exceeding this timeframe.

UPLC-ESI-Q-TOFMS

Both sets of samples were analyzed via ultra-high performance liquid chromatography coupled with electrospray ionization quadrupole time-of-flight mass spectrometry (UPLC-ESI-Q-TOFMS) using an UltiMate 3000 UPLC system (Thermo Scientific) and a Bruker Impact HD Q-TOF mass spectrometer.

Specific chromatographic conditions were employed. Separation was performed on a Waters Atlantis T3 C18 column (3 μm particle size, 2.1 mm × 150 mm dimensions) equipped with a compatible guard column. The mobile phase consisted of (A) methanol with 0.1% acetic acid and (B) water with 0.1% acetic acid. The flow rate was maintained at 200 $\mu L\ min^{-1}$ with an injection volume of 5 μL. The column temperature was set at 50 °C. A 17-min gradient elution program was used as follows: 0-1.5 min: 1% A / 99% B (isocratic); 1.5-8 min: 1-60% A / 99-40% B (linear gradient); 8-10 min: 60-95% A / 40-5% B (linear gradient); 10-12 min: 95-100% A / 5-0% B (linear gradient); 12-14 min: 100% A / 0% B (isocratic); 14-14.5 min: 100-1% A / 0-99% B (linear gradient); 14.5-17 min: 1% A / 99% B (isocratic, re-equilibration).

Analysis utilized negative ESI. Key ESI source parameters were set as: capillary voltage, 4.0 kV; dry gas heater temperature, 200 °C; dry gas flow rate, 5.0 $L\ min^{-1}$; nebulizer gas pressure, 0.4 bar. Mass spectra were acquired in full-scan mode over the *m*/*z* range 50-1500. Data acquisition and processing were controlled by Bruker Compass software (version 4.2). Molecular formula assignment for organic species was performed based on reaction mechanisms and elemental composition constraints, considering detected masses within a ± 5 ppm mass error tolerance. The MS signals of blanks, arising mainly from the impurities in the filter and solvent, were subtracted from those of SOA samples. During initial processing of raw data, peaks resulting from artifacts and background interference were first excluded, including those from substances present on blank filters. Subsequently, for each test sample, the peak with the highest mass spectrometric signal was designated as the base peak, and any peaks within the analytical peak list exhibiting a signal intensity below 0.1% of the base peak intensity were deleted. Following this, the retained mass spectral peaks were constrained by atom counts and elemental ratios, with atomic assignments within a mass error tolerance of ±5 ppm. Specific constraints applied were: $1 \leq {}^{12}C \leq 50$, $2 \leq {}^{1}H \leq 100$, $1 < {}^{16}O \leq 50$, $0.3 \leq H: C \leq 3$, $0.3 \leq O: C \leq 3$. Additionally, the ratio of Double Bond Equivalence (DBE) to the number of C atoms was required to be between 0 and 1. Based on these conditions, the software derived the optimal molecular formulas, i.e., CHO compounds.

Text S4 Mass spectroscopy-related calculations

The volatility of SOA

The volatility of compounds correlates with their molecular mass.[5] Based on this, Li *et al*. developed a predictive method for a compound's saturation mass concentration (C^0_i, μg m^{-3}), given by Equation S4:[6]

$$\log_{10} C_i^0 = \left(n_C^0 - n_c^i\right) b_C - n_O^1 b_O - 2\frac{n_C^i n_O^i}{n_C^i + n_O^i} b_{CO} - n_N^i b_N - n_S^i b_S \tag{S4}$$

Here, n^0_C is the reference number of carbon atoms; n^i_C, n^i_O, n^i_N, and n^i_S represent the number of C, O, N, and S atoms, respectively. b_C, b_O, b_N, and b_S denote the contribution per C, O, N, and S atom to $\log_{10}C^0_i$. b_{CO} is the C-O non-ideality index. The values of these parameters differ for compounds containing different elements; specific values are detailed in Table S5.

Based on saturation mass concentration values, products are categorized into the following four types: VOC ($C^0_i > 3 \times 10^6$ μg m^{-3}), IVOC ($300 < C^0_i < 3 \times 10^6$ μg m^{-3}), SVOC ($0.3 < C^0_i < 300$ μg m^{-3}), LVOC ($3 \times 10^{-4} < C^0_i < 0.3$ μg m^{-3}), ELVOC ($C^0_i < 3 \times 10^{-4}$ μg m^{-3}).[7]

DBE

The Double Bond Equivalent (DBE) represents the total number of rings and double bonds in a compound, quantifying the degree of unsaturation in the molecule. It can be calculated according to Equation S5:[8]

$$DBE = 1 + c + \frac{n - h}{2} \tag{S5}$$

OS$_C$

The oxidation state of carbon (OS$_C$) characterizes the average oxidation level of carbon atoms in an organic molecule and is calculated using Equation S6:[5]

$$OS_C = 2 \times \frac{O}{C} - \frac{H}{C} \tag{S6}$$

171 **Other Figures**

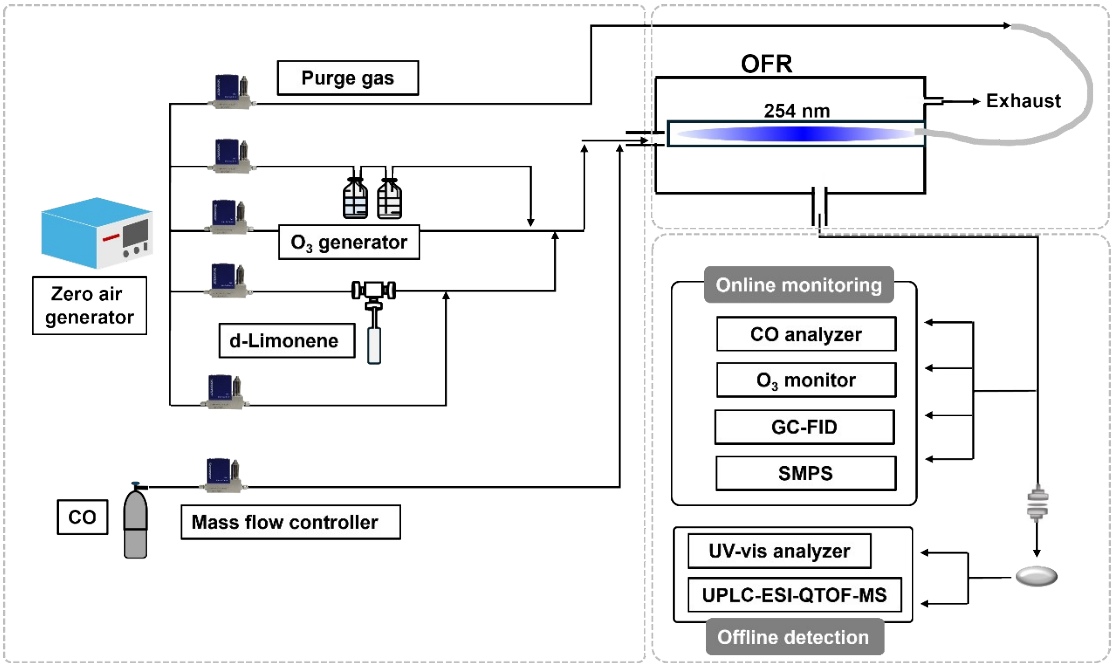

172

173 **Fig. S1** The overall schematic diagram of the OFR.

174

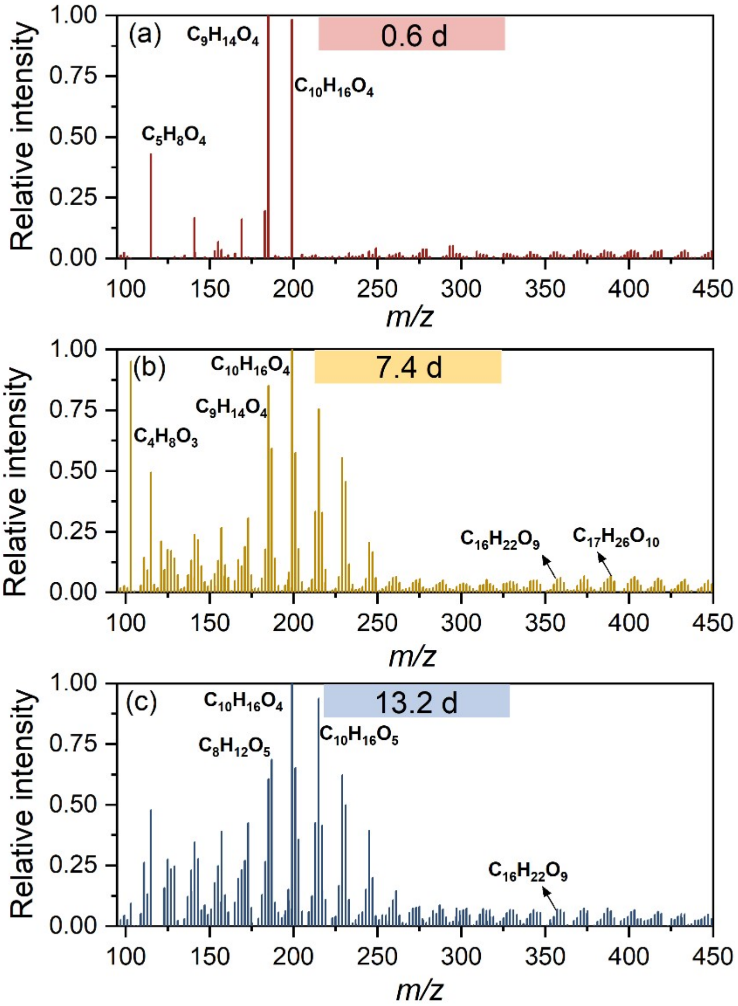

Fig. S2 The average mass spectrum of limonene SOA under typical aging conditions. An average mass spectrum is generated by selecting a chromatographic peak (t_1-t_2) from Total Ion Chromatogram (TIC), then point-by-point averaging all acquired spectra's signal intensities per *m/z*.

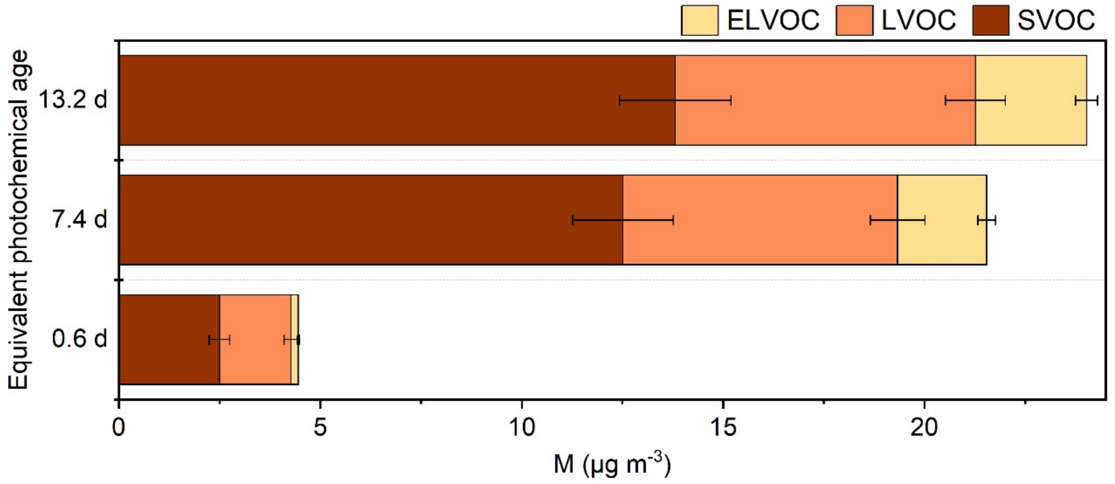

Fig. S3 Concentrations (M, μg m^{-3}) of SVOC, LVOC and ELVOC in representative experiments (M = sum of relative intensities in MS × SOA mass concentration). The error comes from the mass concentration of SOA.

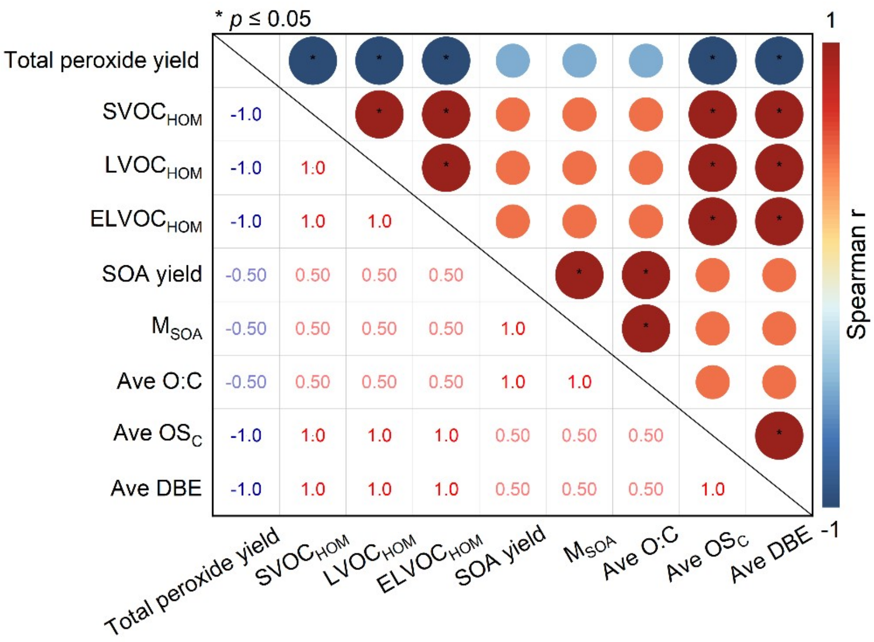

Fig. S4 Spearman correlation matrix of chemical molecules and total peroxide yield. Blue color and numbers mean negative correlations, red color and numbers mean positive correlations. The circle size also indicates the intensity of the correlation.

Other tables

Table S1 Experimental conditions for the OH oxidation of limonene.

Exp.	Equivalent photochemical age (days)	$[\text{limonene}]_0$ (ppb)	$\Delta[\text{limonene}]_0$ (ppb)	M_{SOA} (μg m^{-3})	SOA yield	OH_{exp} (10^{11} molec cm^{-3} s)
D-1	0.6	372 ± 20	372 ± 20	99.5 ± 10.0	4.7 ± 0.9%	0.8
D-2	7.4	372 ± 20	372 ± 20	283.8 ± 28.4	13.4 ± 2.7%	9.6
D-3	8.8	372 ± 20	372 ± 20	235.0 ± 23.5	11.1 ± 2.2%	11.5
D-4	10.3	372 ± 20	372 ± 20	213.8 ± 21.4	10.1 ± 2.0%	13.3
D-5	11.7	372 ± 20	372 ± 20	202.5 ± 20.3	9.5 ± 1.9%	15.2
D-6	13.2	372 ± 20	372 ± 20	160.0 ± 16.0	7.5 ± 1.5%	17.1

Table S2 Peroxides identified at 0.6 d photochemical age.

[M-H][1]	Before[2]	After[2]	[M-H][1]	Before[2]	After[2]	[M-H][1]	Before[2]	After[2]
$C_{19}H_{29}O_9$	0.618%	0.213%	$C_{13}H_{19}O_8$	0.115%	☐	$C_{17}H_{25}O_{11}$	0.044%	☐
$C_{18}H_{25}O_8$	0.306%	0.100%	$C_{19}H_{27}O_{10}$	0.115%	☐	$C_{19}H_{21}O_9$	0.044%	☐
$C_{18}H_{27}O_8$	0.633%	0.246%	$C_{14}H_{23}O_8$	0.113%	☐	$C_{11}H_{11}O_8$	0.043%	☐
$C_{18}H_{27}O_7$	0.477%	0.170%	$C_{13}H_{17}O_4$	0.112%	☐	$C_{14}H_{19}O_{10}$	0.043%	☐
$C_{10}H_{15}O_3$	3.716%	1.101%	$C_{11}H_{17}O_8$	0.109%	☐	$C_{15}H_{21}O_{10}$	0.042%	☐
$C_{10}H_{15}O_4$	18.677%	7.425%	$C_{11}H_{15}O_3$	0.109%	☐	$C_{12}H_{19}O_9$	0.042%	☐
$C_{12}H_{23}O_8$	0.977%	☐	$C_8H_{11}O_7$	0.107%	☐	$C_{18}H_{29}O_{12}$	0.041%	☐
$C_{12}H_{21}O_8$	0.961%	0.341%	$C_{18}H_{23}O_8$	0.107%	☐	$C_{12}H_{21}O_3$	0.040%	☐
$C_{10}H_{17}O_7$	0.813%	0.283%	$C_{12}H_{17}O_8$	0.105%	☐	$C_{21}H_{25}O_{10}$	0.038%	☐
$C_{19}H_{31}O_{10}$	0.620%	0.243%	$C_{11}H_{19}O_9$	0.105%	☐	$C_{22}H_{31}O_9$	0.038%	☐
$C_{20}H_{33}O_{11}$	0.562%	0.193%	$C_{14}H_{23}O_7$	0.104%	☐	$C_4H_5O_5$	0.037%	☐
$C_{12}H_{21}O_9$	0.548%	☐	$C_{21}H_{31}O_{10}$	0.101%	☐	$C_{13}H_{19}O_9$	0.037%	☐
$C_{12}H_{21}O_9$	0.548%	0.208%	$C_{11}H_{17}O_3$	0.100%	☐	$C_6H_{11}O_4$	0.036%	☐
$C_5H_7O_2$	0.438%	0.159%	$C_{21}H_{31}O_9$	0.095%	☐	$C_7H_{13}O_5$	0.035%	☐
$C_{19}H_{31}O_{11}$	0.438%	0.128%	$C_8H_{15}O_3$	0.093%	☐	$C_9H_{17}O_6$	0.033%	☐
$C_{18}H_{29}O_{10}$	0.423%	0.157%	$C_{10}H_{13}O_8$	0.090%	☐	$C_{20}H_{31}O_4$	0.033%	☐
$C_9H_{13}O_7$	0.414%	0.129%	$C_{14}H_{25}O_9$	0.090%	☐	$C_{13}H_{23}O_6$	0.032%	☐
$C_{11}H_7O_{10}$	0.354%	☐	$C_{12}H_{15}O_3$	0.089%	☐	$C_9H_9O_{14}$	0.031%	☐
$C_{20}H_{31}O_{11}$	0.327%	☐	$C_4H_7O_4$	0.088%	☐	$C_9H_7O_2$	0.030%	☐
$C_8H_{13}O_6$	0.295%	0.115%	$C_5H_9O_2$	0.084%	☐	$C_{19}H_{23}O_7$	0.030%	☐
$C_{18}H_{27}O_{10}$	0.292%	☐	$C_{17}H_{21}O_7$	0.084%	☐	$C_4H_5O_6$	0.030%	☐
$C_{16}H_{23}O_9$	0.286%	☐	$C_8H_{15}O_5$	0.083%	☐	$C_8H_5O_7$	0.029%	☐
$C_{16}H_{25}O_8$	0.273%	☐	$C_{18}H_{25}O_{10}$	0.082%	☐	$C_{19}H_{29}O_{12}$	0.026%	☐
$C_{17}H_{27}O_{10}$	0.272%	☐	$C_{15}H_{25}O_8$	0.081%	☐	$C_7H_9O_{13}$	0.026%	☐
$C_{20}H_{29}O_8$	0.258%	☐	$C_{13}H_{11}O_7$	0.077%	☐	$C_{13}H_{23}O_7$	0.025%	☐
$C_8H_7O_2$	0.239%	0.096%	$C_{10}H_{19}O_2$	0.076%	☐	$C_3H_3O_4$	0.024%	☐
$C_5H_5O_2$	0.232%	0.086%	$C_{20}H_{31}O_6$	0.071%	☐	$C_{16}H_{25}O_4$	0.024%	☐
$C_{16}H_{25}O_{10}$	0.208%	☐	$C_{19}H_{29}O_5$	0.070%	☐	$C_{21}H_{33}O_7$	0.024%	☐
$C_{17}H_{25}O_{10}$	0.201%	☐	$C_{12}H_{17}O_3$	0.070%	☐	$C_{16}H_{23}O_{11}$	0.023%	☐
$C_7H_9O_6$	0.198%	0.077%	$C_5H_7O_5$	0.067%	☐	$C_{14}H_{27}O_8$	0.023%	☐
$C_{11}H_{15}O_7$	0.196%	☐	$C_6H_5O_6$	0.064%	☐	$C_{13}H_{21}O_3$	0.023%	☐
$C_9H_{15}O_7$	0.165%	☐	$C_{11}H_{19}O_4$	0.062%	☐	$C_{17}H_{15}O_{12}$	0.023%	☐
$C_{10}H_{17}O_8$	0.157%	☐	$C_{13}H_{21}O_4$	0.060%	☐	$C_{11}H_{21}O_5$	0.022%	☐
$C_{10}H_{19}O_7$	0.149%	☐	$C_{17}H_{25}O_4$	0.060%	☐	$C_{14}H_{25}O_3$	0.022%	☐
$C_{10}H_{15}O_8$	0.147%	☐	$C_{12}H_{19}O_3$	0.058%	☐	$C_{12}H_{15}O_9$	0.021%	☐
$C_{11}H_{21}O_8$	0.134%	☐	$C_{15}H_{23}O_4$	0.056%	☐	$C_{17}H_{15}O_{13}$	0.021%	☐
$C_7H_{11}O_6$	0.132%	☐	$C_{23}H_{31}O_8$	0.055%	☐	$C_{17}H_{21}O_{11}$	0.020%	☐
$C_4H_3O_3$	0.130%	☐	$C_{13}H_{19}O_3$	0.053%	☐	$C_{12}H_5O_9$	0.019%	☐
$C_9H_{15}O_2$	0.129%	☐	$C_{13}H_{15}O_9$	0.053%	☐	$C_9H_{13}O_8$	0.019%	☐

[M-H][1]	Before[2]	After[2]	[M-H][1]	Before[2]	After[2]	[M-H][1]	Before[2]	After[2]
$C_{18}H_{23}O_9$	0.122%	☐	$C_{19}H_{27}O_{11}$	0.052%	☐	$C_{15}H_{25}O_4$	0.019%	☐
$C_{12}H_{15}O_4$	0.119%	☐	$C_{15}H_{23}O_{10}$	0.051%	☐	$C_{20}H_{23}O_9$	0.019%	☐
$C_9H_{11}O_7$	0.118%	☐	$C_{14}H_{23}O_4$	0.049%	☐	$C_{16}H_{13}O_{13}$	0.019%	☐
$C_{15}H_{23}O_9$	0.116%	☐	$C_{13}H_{13}O_6$	0.049%	☐	$C_{12}H_9O_8$	0.018%	☐
$C_{12}H_{19}O_4$	0.116%	☐	$C_{15}H_{17}O_9$	0.048%	☐	$C_{16}H_{13}O_{12}$	0.018%	☐

[1] Molecules (relative intensity lower than 40%) after the iodometry are identified as peroxides.

[2] Relative intensity of a molecule = absolute intensity of the molecule in the mass spectrum / total intensity of all molecules.

Table S3 Peroxides identified at 13.2 d photochemical age.

[M-H]	Before	After	[M-H]	Before	After	[M-H]	Before	After
$C_{10}H_{15}O_5$	3.318%	1.120%	$C_{18}H_{21}O_9$	0.070%	□	$C_{14}H_{15}O_{12}$	0.010%	□
$C_9H_{13}O_5$	2.306%	0.902%	$C_{13}H_{11}O_8$	0.069%	□	$C_{14}H_{11}O_{11}$	0.010%	□
$C_8H_{11}O_6$	1.263%	0.114%	$C_8H_5O_5$	0.063%	□	$C_{19}H_{33}O_{11}$	0.010%	□
$C_8H_9O_5$	1.259%	□	$C_{12}H_9O_8$	0.060%	□	$C_{16}H_{27}O_{10}$	0.010%	□
$C_{10}H_{17}O_5$	0.518%	□	$C_{16}H_{19}O_7$	0.060%	□	$C_{15}H_{11}O_{10}$	0.009%	□
$C_9H_9O_6$	0.438%	□	$C_6H_3O_5$	0.058%	□	$C_{21}H_{37}O_{10}$	0.009%	□
$C_{10}H_{17}O_6$	0.359%	□	$C_{13}H_{21}O_8$	0.056%	□	$C_{17}H_{25}O_5$	0.008%	□
$C_8H_{13}O_5$	0.347%	□	$C_{12}H_{21}O_8$	0.053%	□	$C_{13}H_7O_{10}$	0.008%	□
$C_9H_{15}O_5$	0.310%	□	$C_{12}H_9O_7$	0.049%	□	$C_{17}H_{29}O_7$	0.008%	□
$C_{14}H_{17}O_7$	0.259%	□	$C_6H_3O_4$	0.043%	□	$C_{14}H_9O_{10}$	0.008%	□
$C_{14}H_{17}O_8$	0.255%	□	$C_{13}H_{21}O_9$	0.040%	□	$C_{18}H_{31}O_8$	0.008%	□
$C_{13}H_{15}O_7$	0.224%	□	$C_{19}H_{29}O_7$	0.036%	□	$C_{10}H_{17}O_{18}$	0.008%	□
$C_9H_{15}O_6$	0.214%	□	$C_{20}H_{27}O_9$	0.036%	□	$C_{12}H_{23}O_8$	0.008%	□
$C_8H_{13}O_6$	0.213%	□	$C_9H_7O_7$	0.034%	□	C_5HO_5	0.007%	□
$C_{10}H_9O_5$	0.211%	□	$C_{20}H_{33}O_8$	0.034%	□	$C_{18}H_{31}O_{11}$	0.007%	□
$C_{12}H_{13}O_7$	0.193%	□	$C_{19}H_{19}O_{12}$	0.034%	□	$C_{20}H_{33}O_7$	0.007%	□
$C_{14}H_{15}O_8$	0.177%	□	$C_{18}H_{29}O_{12}$	0.032%	□	$C_{14}H_9O_{11}$	0.006%	□
$C_9H_7O_5$	0.175%	□	$C_6H_3O_3$	0.030%	□	$C_{22}H_{39}O_5$	0.006%	□
$C_{11}H_{11}O_6$	0.170%	□	$C_5H_3O_5$	0.030%	□	$C_{10}H_{11}O_{17}$	0.006%	□
$C_{12}H_{13}O_6$	0.161%	□	$C_{11}H_{19}O_5$	0.028%	□	$C_{14}H_{25}O_8$	0.005%	□
$C_{10}H_{17}O_7$	0.152%	□	$C_{20}H_{33}O_4$	0.028%	□	$C_{21}H_{35}O_9$	0.005%	□
$C_{11}H_{11}O_7$	0.151%	□	$C_{21}H_{29}O_{10}$	0.028%	□	$C_{19}H_{33}O_8$	0.005%	□
$C_9H_7O_6$	0.149%	□	$C_{12}H_{13}O_{11}$	0.027%	□	$C_9H_{11}O_{18}$	0.005%	□
$C_{16}H_{19}O_9$	0.143%	□	$C_{16}H_{25}O_6$	0.026%	□	$C_{13}H_{23}O_7$	0.005%	□
$C_{17}H_{27}O_9$	0.127%	□	$C_{11}H_5O_8$	0.020%	□	$C_{14}H_{11}O_{12}$	0.005%	□
$C_{13}H_{17}O_6$	0.123%	□	$C_{16}H_{27}O_9$	0.017%	□	$C_6H_3O_2$	0.004%	□
$C_{19}H_{29}O_9$	0.122%	0.018%	$C_{15}H_{15}O_{12}$	0.017%	□	$C_{21}H_{31}O_8$	0.004%	□
$C_{13}H_{13}O_7$	0.122%	□	$C_7H_3O_5$	0.017%	□	$C_{20}H_{37}O_{10}$	0.004%	□
$C_{10}H_9O_4$	0.122%	□	$C_{16}H_{27}O_8$	0.017%	□	$C_{18}H_{29}O_6$	0.004%	□
$C_{11}H_{11}O_5$	0.119%	□	$C_{15}H_{21}O_5$	0.016%	□	$C_9H_9O_{18}$	0.004%	□
$C_9H_7O_4$	0.111%	□	$C_{12}H_{19}O_4$	0.015%	□	$C_9H_7O_{14}$	0.004%	□
$C_{24}H_{41}O_6$	0.109%	□	$C_{19}H_{29}O_6$	0.015%	□	$C_{14}H_{25}O_7$	0.004%	□
$C_{11}H_{13}O_4$	0.102%	□	$C_{15}H_{23}O_5$	0.015%	□	$C_{15}H_{15}O_{13}$	0.004%	□
$C_{18}H_{25}O_8$	0.102%	0.040%	$C_{15}H_{11}O_{11}$	0.015%	□	□		□
$C_{18}H_{27}O_8$	0.100%	0.033%	$C_7H_3O_4$	0.014%	□	□		□
$C_{18}H_{29}O_9$	0.095%	□	$C_{16}H_{13}O_{11}$	0.014%	□	□		□
$C_{13}H_{15}O_5$	0.095%	□	$C_{17}H_{15}O_{12}$	0.013%	□	□		□
$C_{12}H_{13}O_5$	0.094%	□	$C_{20}H_{29}O_7$	0.013%	□	□		□
$C_{11}H_9O_8$	0.090%	□	$C_{22}H_{37}O_9$	0.013%	□	□		□

[M-H]	Before	After	[M-H]	Before	After	[M-H]	Before	After
$C_{20}H_{25}O_{11}$	0.086%	☐	$C_{14}H_{11}O_8$	0.012%	☐	☐		☐
$C_{17}H_{27}O_{11}$	0.080%	☐	$C_{16}H_{27}O_7$	0.011%	☐	☐		☐
$C_{17}H_{19}O_9$	0.077%	☐	$C_9H_{17}O_4$	0.011%	☐	☐		☐
$C_{19}H_{21}O_{10}$	0.076%	☐	$C_{12}H_{21}O_5$	0.011%	☐	☐		☐
$C_{18}H_{19}O_{10}$	0.076%	☐	$C_9H_{17}O_5$	0.011%	☐	☐		☐
$C_{14}H_{13}O_8$	0.075%	☐	$C_{21}H_{31}O_9$	0.011%	☐	☐	☐	☐

Table S4 Parameters of peroxide with inferred chemical structures.

Molecular Formula [M]	[M-H]	Molar mass	Error	Retention time
□	□	(g mol^{-1})	(ppm)	(min)
$C_8H_{12}O_6$	$C_8H_{11}O_6$	203.0558	1.3	9.7
$C_9H_{14}O_5$	$C_9H_{13}O_5$	201.0768	0.4	8.7
$C_9H_{14}O_7$	$C_9H_{13}O_7$	233.0658	4.0	11.7
$C_{10}H_{16}O_3$	$C_{10}H_{15}O_3$	183.1019	4.2	11.7
$C_{10}H_{16}O_4$	$C_{10}H_{15}O_4$	199.0970	3.0	11.2
$C_{10}H_{16}O_5$	$C_{10}H_{15}O_5$	215.0926	-0.4	10.8
$C_{10}H_{16}O_8$	$C_{10}H_{15}O_8$	263.0771	0.4	8.9
$C_{10}H_{18}O_7$	$C_{10}H_{17}O_7$	249.0968	4.6	9.9
$C_{10}H_{18}O_8$	$C_{10}H_{17}O_8$	265.0938	-3.3	11.9
$C_{18}H_{26}O_8$	$C_{18}H_{25}O_8$	369.1560	-1.2	11.6
$C_{18}H_{28}O_7$	$C_{18}H_{27}O_7$	355.1747	4.2	11.8
$C_{18}H_{28}O_8$	$C_{18}H_{27}O_8$	371.1709	0.6	10.5
$C_{18}H_{30}O_6$	$C_{18}H_{29}O_6$	341.1974	-1.4	10.8
$C_{19}H_{30}O_9$	$C_{19}H_{29}O_9$	401.1815	0.6	11.5

Table S5 Parameter values used to calculate the saturated mass concentration of different compounds[6]

Types[1]	n^0_C	b_C	b_O	b_{CO}	b_N	b_S
CH	23.80	0.4861	/	/	/	/
CHO	22.66	0.4481	1.656	-0.7790	/	/
CHN	24.59	0.4066	/	/	0.9619	/
CHON	24.13	0.3667	0.7732	-0.07790	1.114	/
CHOS	24.06	0.3637	1.327	-0.3988	/	0.7579
CHONS	28.50	0.3848	1.011	0.2921	1.053	1.316

[1] Take CHONS compounds as an example. The letters in them indicate that this type of compound contains elements C, H, O, N, and S.

References

1. J. Mao, X. Ren, W. H. Brune, J. R. Olson, J. H. Crawford, A. Fried, L. G. Huey, R. C. Cohen, B. Heikes, H. B. Singh, D. R. Blake, G. W. Sachse, G. S. Diskin, S. R. Hall and R. E. Shetter, Airborne measurement of OH reactivity during INTEX-B, *Atmos. Chem. Phys.*, 2009, **9**, 163-173.
2. Q. Liu, J. Liggio, K. Li, P. Lee and S.-M. Li, Understanding the impact of relative humidity and coexisting soluble iron on the OH-initiated heterogeneous oxidation of organophosphate flame retardants, *Environ. Sci. Technol.*, 2019, **53**, 6794-6803.
3. R. Atkinson and J. Arey, Atmospheric degradation of volatile organic compounds, *Chem. Rev.*, 2003, **103**, 4605-4638.
4. Z. Peng and J. L. Jimenez, Radical chemistry in oxidation flow reactors for atmospheric chemistry research, *Chem. Soc. Rev.*, 2020, **49**, 2570-2616.
5. J. H. Kroll, N. M. Donahue, J. L. Jimenez, S. H. Kessler, M. R. Canagaratna, K. R. Wilson, K. E. Altieri, L. R. Mazzoleni, A. S. Wozniak, H. Bluhm, E. R. Mysak, J. D. Smith, C. E. Kolb and D. R. Worsnop, Carbon oxidation state as a metric for describing the chemistry of atmospheric organic aerosol, *Nat. Chem.*, 2011, **3**, 133-139.
6. Y. Li, U. Pöschl and M. Shiraiwa, Molecular corridors and parameterizations of volatility in the chemical evolution of organic aerosols, *Atmos. Chem. Phys.*, 2016, **16**, 3327-3344.
7. N. M. Donahue, S. A. Epstein, S. N. Pandis and A. L. Robinson, A two-dimensional volatility basis set: 1. organic-aerosol mixing thermodynamics, *Atmos. Chem. Phys.*, 2011, **11**, 3303-3318.
8. S. L. Blair, A. C. MacMillan, G. T. Drozd, A. H. Goldstein, R. K. Chu, L. Paša-Tolić, J. B. Shaw, N. Tolić, P. Lin, J. Laskin, A. Laskin and S. A. Nizkorodov, Molecular characterization of organosulfur compounds in biodiesel and diesel fuel secondary organic aerosol, *Environ. Sci. Technol.*, 2017, **51**, 119-127.